Glacier Velocity Measurements with Landsat-8 Oli Data
Case Study on Yanong Glacier in Tibetan Plateau of China

Zhang, Jing; Jia, Li; Menenti, Massimo; Ren, Shaoting; Zhang, Jingxiao

DOI
10.1109/IGARSS.2019.8898864

Publication date
2019

Document Version
Final published version

Published in
2019 IEEE International Geoscience and Remote Sensing Symposium, IGARSS 2019 - Proceedings

GLACIER VELOCITY MEASUREMENTS WITH LANDSAT-8 OLI DATA: CASE STUDY ON YANONG GLACIER IN TIBETAN PLATEAU OF CHINA

Jing Zhang[1, 2], *Li Jia*[1 *], *Massimo Menenti*[1, 3], *Shaoting Ren*[1, 2], *Jingxiao Zhang*[1, 2]
[1] State Key Laboratory of Remote Sensing Science, Institute of Remote Sensing and Digital Earth, Chinese Academy of Sciences, Beijing, 100101, China; [2] University of Chinese Academy of Sciences, Beijing, 100049, China; [3]Faculty of Civil Engineering and Earth Sciences (CITG), Delft University of Technology (TUD), Post Box 5048, 2628 CN Delft, The Netherlands,
* Corresponding author: jiali@radi.ac.cn; zhangjing2015@radi.ac.cn

ABSTRACT

Mountain glaciers are sensitive to climate change and are thus relevant indicators of regional climate variability. In order to understand the dynamics of glaciers, retrieving glacier surface velocity is valuable in understanding physical processes in glaciers. We apply an image cross-correlation algorithm in the frequency domain to derive glacier velocity on the Yanong glacier between 2013 and 2018. The results indicate that the flow patterns are related to the terrain complexity. Yanong Glacier maximum velocity was 168 m/year at the elevation around 4700 meters. The surface velocity exceeded 100 m/year above the elevation of 4200 m, while above 5000 m the surface velocity fluctuated around 60 m/year along the main stream.

Index Terms— Yanong glacier, cross-correlation, surface velocity

1. INTRODUCTION

In the 20th century climate has caused dramatic variations in mountain glaciers in general, and in the Tibetan Plateau in particular. Mountain glaciers are not only the freshwater suppliers in the Tibetan Plateau but also climate response indicators[1]. Gaining a better understanding of mountain glacier dynamics in space and time is therefore of great importance. Glacier velocity is a key factor in glacier dynamical processes such as glacier surges, development of glacier lakes, lake-outburst floods, and glacier debris-flow hazards. Better satellite imagery coverage and repeated acquisitions significantly improved our ability to measure large scale and long term surface movement. Glacier velocity monitoring by remote sensing techniques is feasible globally[2-5], which has enormous potential to broaden our knowledge in glacier flow.

The phase correlation algorithm used in COSI-Corr (hereafter referred to as COSI-Corr) is a robust matching method for global-scale mapping and monitoring of glacier velocities[6]. Several studies have used this method to observe the dynamics of individual glaciers[7,8]. In this study, the cross-correlation algorithm in the frequency domain was applied on multi-temporal Landsat 8 OLI images to construct glacier velocity fields from 2013 to 2018 in Yanong glacier in Tibetan Plateau of China.

2. STUDY AREA

The Yanong Glacier (GLIMS ID is G096657E29334N) is located in the Kangri Karpo Mountains of the Southeast Tibet Plateau. Yanong glacier is a maritime glacier, which captures the warm and humid moisture carried by the southwest monsoon penetrates into the Tibetan Plateau[9]. During winter and spring, the westerly jet is blocked by the Tibetan Plateau and splits into two parts; the southern branch forms a trough in the Kangri Karpo Mountains after avoiding the Himalayas. Moisture derived from the Bay of Bengal is delivered to this trough, causing heavy snowfalls and therefore developing maritime glaciers[10]. Glacier velocity is high and surface melting is intense. As shown in Figure 1 Yanong Glacier is about 32 km in length, terminating in a proglacial lake. According to [11], during summer, the temperatures in this region rise continuously. Studying the variation of maritime glaciers in this region helps to improve the understanding of the relationship between glaciers and southwest monsoon.

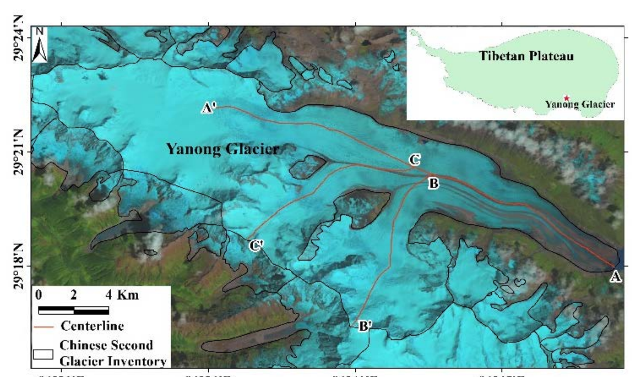

Figure 1. Location of Yanong glacier. The red line is the centerline of Yanong Glacier. The black line is the glacier border from the Chinese Second Glacier Inventory.

3. DATA

In this study, we utilized Landsat-8 OLI images acquired in the period 2013-2018 to estimate the glacier surface velocity over the Yanong Glacier. Landsat-8 provides high-quality moderate-resolution imagery, available from the U.S. Geological Survey. The Level 1T image data product is orthorectified, radiometric and geometric corrected and transformed to UTM projection. We used 33 images in total and generated 179 maps of displacement retrievals, using different combinations of acquisition dates. All the panchromatic images (15 m resolution) used in this study were in the same path/row (134/40), which is a very suitable source for tracking glacier flow velocity.

4. METHOD

4.1. Glacier surface displacement

Glaciers surface displacement were quantified by calculating co-registration and correlation of the optical imagery using the software package COSI-Corr (Co-registration of Optically Sensed Images and Correlation), developed by Leprince[12]. Horizontal displacements along the East/West (E/W) and North/South (N/S) direction were measured using an 8 × 8 (pixels) window as the initial search window and a 32 × 32 (pixels) window as the final window. A coherence mask was applied to select segments of the spectrum where the phase information was reliable. The mask parameter (coherence in the frequency domain) was set to be larger than 0.9. Finally, we obtained the displacement maps at a resolution of 15 m (a sliding step set as one pixel for the correlation window). Each image was combined with six images at different times to calculate displacements to decrease the mismatches due to e.g. cloud cover, snow cover and melting glaciers. We refer to the set of image pairs overlapping the same period in time as "stack". The glacier velocity v was estimated using Eq.(1):

$$v = \frac{D}{A_i} \qquad (1)$$

where D (m) is the displacement measured between each paired images; A_i is the interval between the paired images in number of days. The unit of velocity is then m/day. For easier comparison with other studies, we convert the unit to m/year by multiplying the averaged velocity by 365 days in one year. Thereafter we refer to the mean annual velocity as stack velocity.

4.2. Accuracy Estimation

Due to the inaccessible study region, it was difficult to directly evaluate the results of the COSI-Corr method. Taking into account that the off-glacier area should not move, the displacement retrievals in the off-glacier area is generally regarded as a reference to evaluate the estimated velocities. The error of the observed velocities in the off-glacier area is[13]:

$$\sigma_{off} = \sqrt{SE^2 + MEAN^2} \qquad (2)$$

σ_{off} is the error of off-glacier area velocity, MEAN is the mean stack velocity. SE is the standard error of the mean velocity, which provides a measure for the corresponding random uncertainty[13]:

$$SE = \frac{STD}{\sqrt{N_{off}}} \qquad (3)$$

where STD is the standard deviation of the off-glacier area velocity. N_{off} is the number of pixels in the sampled off-glacier area. In our case-study STD was 5.42 m/year and σ_{off} was 6.47 m/year.

5. RESULTS

Glaciers with complex terrain and tributary flows are frequent in high-mountain regions. Figure 3 displays the stack velocity of the velocity fields in the Yanong Glacier derived from 179 displacement retrievals. In general, larger portions of the glacier flowed faster than the smaller portions. The glacier velocity accelerated from the glacier snout to the upper area. The maximum velocity at about 4700 m, reached 168 m/year. According to the off- glacier area statistics, the incertitude of the velocity results was approximately 6.47 m/year. The error on displacement was less than half pixel. The A-A', B-B', C-C' profile is along the centerline location shown by the red line in Figure 1 and Figure 3.

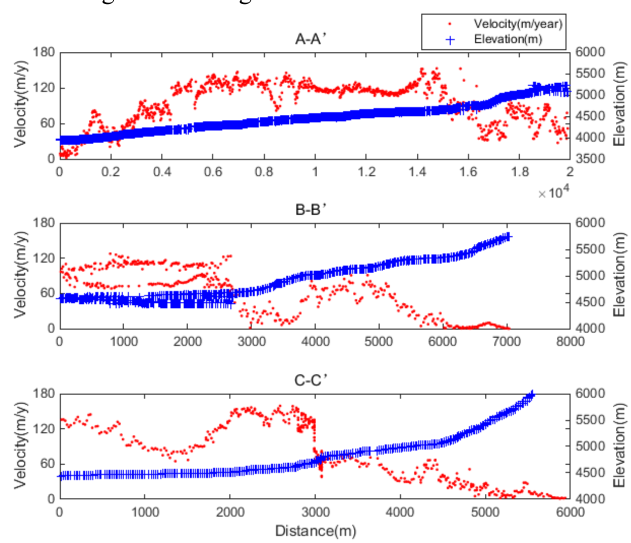

Figure 2. Stack result of Annual glacier velocity profiles along the centerline (A-A', B-B', C-C') of the Yanong Glacier. The centerline location is shown the red line in Figure 1 and Figure 3.

As can be seen in Figure 2, the glacier velocity of Yanong Glacier is highest along the A-A' profile (the main stream of the glacier). The first velocity peak is at approximately 1.3 km from the terminus, with a speed of 70 m/year. In the ablation zone speed increases with elevation. On the contrary, in the accumulation zone, the speed is decreasing with elevation. The surface velocity exceeded 100 m/year above the elevation of 4200 m, while above 5000 m the surface velocity fluctuated around 60 m/year along the main stream. The second peak velocity is at 14.6 km from the end of glacier tone approximately 120 m/year, with the elevation between 4600 and 4700 m. This can be due to glacier melting and elevation change. The B-B’ and C-C’ profiles apply to the tributary glaciers feeding the main stream. As shown in the B-B’ profile, the maximum velocity reached 120 m/year, while in the C-C’ profile the maximum velocity was about 160 m/year, located at the bend of the glacier. At the lower junction point, glacier velocity was about 130 m/year.

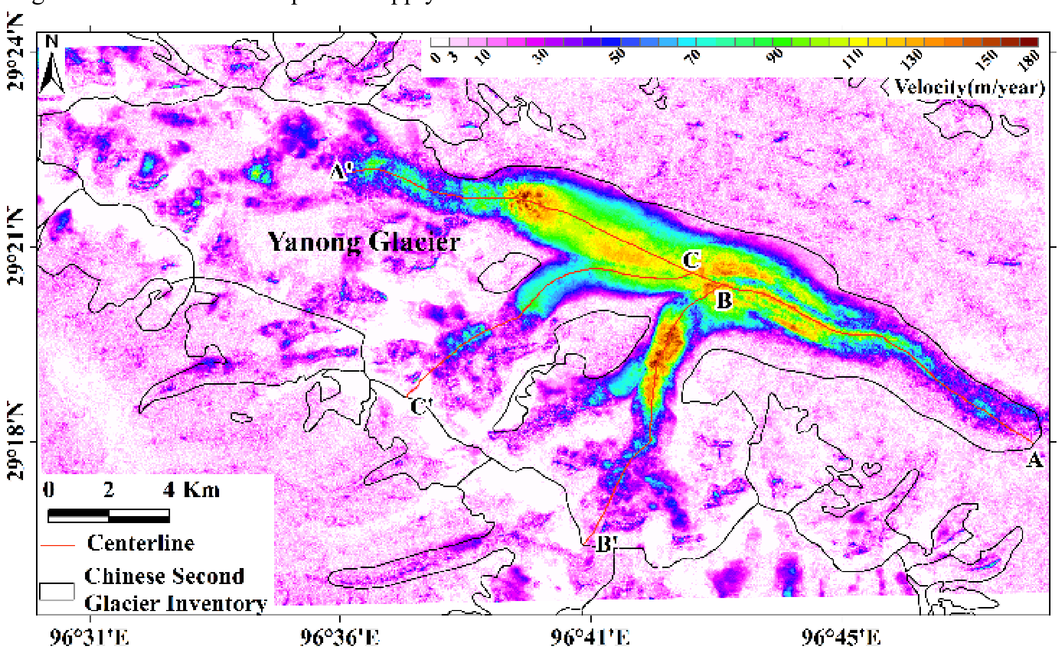

Figure 3. Stack velocity of the annual velocity field in Yanong Glacier from 2013-2018.

6. CONCLUSIONS

This study retrieved glacier surface velocity of Yanong Glacier between 2013 and 2018 using Landsat-8 OLI images. The stack velocities result were calculated using Cosi-Corr method based on 179 maps of glacier surface displacement. Yanong Glacier maximum velocity was 168 m/year at the elevation around 4700 meters, and the velocity exceeded 100 m/year between 4200 and 4800 m elevation. According to the spatial pattern of retrieved glacier velocity, the tributary glaciers contribute to the main glacier velocity. More studies on this glacier, as well as more glacier cases, using longer observation records are in-progress.

7. ACKNOWLEDGEMENT

This work was jointly supported by the projects funded by the Strategic Priority Research Program of the Chinese Academy of Sciences (Grant No. XDA19030203, XDA19070102), the International Partnership Program of Chinese Academy of Sciences (Grant No. 131C11KYSB20160061), the National Natural Science Foundation of China project (Grant No. 91737205), CAS "Light of West China" Program and the SAFEA Long-Term-Projects of the 1000 Talent Plan for High-Level Foreign Experts (Grant No. WQ20141100224).

8. REFERENCES

[1] Change C, "Intergovernmental Panel on Climate Change (IPCC) ", *Encyclopedia of Energy Natural Resource & Environmental Economics*, vol. 26, no. 2, pp.48-56, 2013.

[2] F. Paul, T. Strozzi, T. Schellenberger, and A. Kääb, "The 2015 Surge of Hispar Glacier in the Karakoram," Remote Sens-Basel, vol. 9, no. 9, 2017.

[3] X. Fu, Z. Li, and J. Zhou, "Characterizing the surge behavior of Alakesayi Glacier in the West Kunlun Shan, Northwestern Tibetan Plateau, from remote-sensing data between 2013 and 2018," J Glaciol, vol. 65, no. 249, pp. 168-172, 2019.

[4] T. Strozzi, F. Paul, A. Wiesmann, T. Schellenberger, and A. Kääb, "Circum-Arctic Changes in the Flow of Glaciers and Ice Caps from Satellite SAR Data between the 1990s and 2017," Remote Sens-Basel, vol. 9, no. 9, 2017.

[5] A. Dehecq, N. Gourmelen, and E. Trouve, "Deriving large-scale glacier velocities from a complete satellite archive: Application to the Pamir–Karakoram–Himalaya," Remote Sens Environ, vol. 162, pp. 55-66, 2015.

[6] T. Heid and A. Kaab, "Evaluation of existing image matching methods for deriving glacier surface displacements globally from optical satellite imagery," (in English), *Remote Sensing of Environment*, vol. 118, pp. 339-355, Mar 15 2012.

[7] Y. L. Sun, L. M. Jiang, L. Liu, Y. F. Sun, and H. S. Wang, "Spatial-Temporal Characteristics of Glacier Velocity in the

Central Karakoram Revealed with 1999-2003 Landsat-7 ETM+ Pan Images," *Remote Sensing*, vol. 9, no. 10, pp.1064-, Oct 2017.
[8] D. Scherler, S. Leprince, and M. Strecker, "Glacier-surface velocities in alpine terrain from optical satellite imagery—Accuracy improvement and quality assessment," *Remote Sensing of Environment*, vol. 112, no. 10, pp. 3806-3819, 2008.
[9] W. Yang, T. Yao, B. Xu, G. Wu, L. Ma, and X. Xin, "Quick ice mass loss and abrupt retreat of the maritime glaciers in the Kangri Karpo Mountains, southeast Tibetan Plateau," *Science Bulletin*, vol. 53, no. 16, pp. 2547-2551, 2008.
[10] K. Wu , S Liu , Z. Jiang , J. Xu, J. Wei, W. Guo, "Recent glacier mass balance and area changes in the Kangri Karpo Mountains from DEMs and glacier inventories," *The Cryosphere*, vol.12, no.1, pp.103-121, 2018.
[11] W. Wang, T. Yao , and X. Yang, "Variations of glacial lakes and glaciers in the Boshula mountain range, southeast Tibet, from the 1970s to 2009," *Annals of Glaciology*, vol. 52, no.58, pp.9-17, 2017.
[12] S. Leprince, "Co-Registration of Optically Sensed Images and Correlation (COSI-Corr): an Operational Methodology for Ground Deformation Measurements," *IEEE International Geoscience & Remote Sensing Symposium IEEE*, 2008.
[13] T. G.-R. Koblet, I; Zemp, M; Jansson, P; Thee, P; Haeberli, W; Holmlund, P, "Reanalysis of multi-temporal aerial images of Storglaciären, Sweden (1959-99) - Part 1: Determination of length, area, and volume changes," *The Cryosphere*, vol. 4, no. 3, pp. 333-343, 2010.